Chemistry–A European Journal
Research Article
doi.org/10.1002/chem.202200953
Chemistry Europe
European Chemical Societies Publishing
www.chemeurj.org



# Development of a Bacterial Enzyme-Based Biosensor for the Detection and Quantification of Selenate

Mozhgan Khorasani Motlagh,[a] Meissam Noroozifar,[a] Rana N. S. Sodhi,[b] and Heinz-Bernhard Kraatz*[a, c]

**Abstract:** An enzymatic biosensor has been developed for the determination of selenate ($SeO_4^{2-}$), in which selenate reductase (SeR) is chemically attached to a gold disk electrode by lipoic acid *N*-hydroxysuccinimide ester as linker, allowing the catalytic reduction of the $SeO_4^{2-}$ to $SeO_3^{2-}$. Modification of the gold electrode was characterized by X-ray photoelectron spectroscopy (XPS), time-of-flight secondary ion mass spectroscopy (ToF-SIMS), and electrochemistry. Cyclic voltammetry (CV) and differential pulse voltammetry (DPV) measurements were performed in different buffers for selenate determination. Under optimum conditions, the calibration curve was linear over the range 7.0–3900.0 $\mu g L^{-1}$ with limits of detection and quantification of 4.97 and 15.56 $\mu g L^{-1}$, respectively. The possible interference of the relevant oxyanions $SO_4^{2-}$, $NO_3^-$, $NO_2^-$, $PO_4^{3-}$ and $AsO_4^{3-}$ in the determination of $SeO_4^{2-}$ was studied. Finally, the proposed biosensor was used to determine $SeO_4^{2-}$ with recovery between 95.2 and 102.4% in different real water samples.

## Introduction

Anthropomorphic activities, such as mining operations and the combustion of fossil fuels, as well as natural processes, including volcanic eruptions, release selenium into the environment as the soluble oxyanions selenate, $SeO_4^{2-}$, and selenite, $SeO_3^{2-}$.[1,2] The bioaccumulation and associated toxicity of inorganic Se oxyanions and organoselenium has led to wide spread concern about environmental selenium contamination and its effects on ecosystems.[3–7] Studies on *'algae'* indicate a high degree of toxicity of $SeO_3^{2-}$.[8] The higher and uptake of selenite versus selenate has also been well documented.[9]

Feeding studies of rats with $SeO_3^{2-}$ and $SeO_4^{2-}$ laced water indicated a higher toxicity of $SeO_3^{2-}$.[10] What is now known is that Se oxyanions interfere with intracellular detoxifications of reactive oxygen species (ROS) and the generation of additional ROS.[11] Selenite is a substrate for calf thymus thioredoxin reductase and thioredoxin and elicits a large non-stoichiometric oxidation of nicotinamide adenine dinucleotide phosphate hydrogen (NADPH) in the presence of oxygen.[12] The c-Jun N-terminal kinase (JNK) signaling pathway is involved in sodium selenite-induced apoptosis mediated by reactive oxygen in HepG2 cancer cells.[13] In addition, recent studies by Bao et al. suggest the reduction of selenite to selenium nanoparticles in vivo.[14]

While the recommended oral uptake of Se varies from country to country, recommended levels vary between 50 and 70 μg/day. Due to health concerns, the recommended upper limits for Se uptake is 400 μg/day.[15] The World Health Organization (WHO) suggested the maximum limit of Se in drinking water to be 10 $\mu g L^{-1}$.[16] Given the potential health impact, efficient analysis of Se is critical and specifically the determination of Se oxyanions remains a significant analytical challenge. Selenium has been determined by various analytical methods such as atomic absorption spectroscopy (AAS),[17,18] high-performance liquid chromatography-inductively coupled plasma mass spectrometry (HPLC-ICP-MS),[19] gas chromatography (GC),[20] catalytic spectrophotometry,[21] and different electroanalytical techniques.[22] Also, some hyphenated techniques were used for speciation of Se oxides. For examples, Goldberg et al. was used ion chromatography coupled with hydride generation atomic absorption spectrometry (IC-HG-ABS) for simultaneously determining inorganic $Se^{IV}$ and $Se^{VI}$.[23] Sanchez-Rodas et al. developed a complex coupling system of HPLC, thermoreduction, hydride generation and atomic fluorescence spectrometry (HPLC-TR-HG-AFS0 for speciation of the selenite, selenate and selenoamino acids such as selenocysteine, selenomethylselenocysteine and selenomethionine.[24] Bettazzi et al. reported a fluorescence emission spectroscopy technique for sensing of selenite and selenate using two acridine-based polyamine ligands.[25] Among these reported methods, analyses by HPLC, GC, and AAS as well as hyphenated methods have shown good sensitivity and allow the quantification of selenate. But their application in the field is limited by their complexity and expense. In contrast, electrochemical methods are compact, simple operation, sensitive, fast, low cost, reliable devices and offer an alternative for the determination of Se.[26–33] Reported methods are focused on $SeO_3^{2-}$

[a] *Dr. M. K. Motlagh, Dr. M. Noroozifar, Prof. H.-B. Kraatz*
*Department Physical and Environmental Sciences*
*University of Toronto Scarborough*
*1265 Military Trail, Toronto, M1C1A4, Ontario (Canada)*
*E-mail: bernie.kraatz@utoronto.ca*
[b] *Dr. R. N. S. Sodhi*
*Ontario Centre for Characterisation of Advanced Materials*
*Department of Chemical Engineering & Applied Chemistry*
*University of Toronto*
*2200 College Street, Toronto, M5S 3E5,Ontario (Canada)*
[c] *Prof. H.-B. Kraatz*
*Department of Chemistry, University of Toronto*
*280 St. George St., Toronto, M5S 3H6, Ontario (Canada)*

*Supporting information for this article is available on the WWW under https://doi.org/10.1002/chem.202200953*

($Se^{IV}$) and use different working electrodes such as mercury, carbon, silver, platinum and gold materials.[23] Other electrochemical approaches based on cathodic and anodic stripping voltammetry, followed by square-wave and differential pulse voltammetry techniques were reported.[23,28–33]

This is in contrast to the approach outlined in this contribution, in which selenate reductase (SeR) is used as a biorecognition element. SeR is a soluble periplasmic enzyme belonging to the DMSO reductase family of molybdenum enzymes that catalyzes the two-electron reduction of selenate to selenite[34] in acetic medium according to:

$$SeO_4^{2-} + 2e^- + 2H^+ \rightarrow SeO_3^{2-} + H_2O \quad (1)$$

Studies by Debieux et al. show that selenate reduction and thus detoxification of selenium ultimately results in the formation of intracellular biogenic Se deposits that are associated with the Se factor A protein.[35] This supports earlier work by Bébien et al. showing that the selenate reductase of *Escherichia coli* displays discrete intracellular Se-containing microstructures.[36] Se nanostructures were also observed by Tan et al. in *Streptomyces* sp. ES2-5.[37] The enzyme selenate reductase from *Thauera selenatis*[34,38,39] is a trimeric $\alpha\beta\gamma$ complex with an apparent molecular weight of 160 kDa, which has one molybdenum, approximately three iron–sulfur clusters and a single cytochrome b group per $\alpha\beta\gamma$ complex. Careful and detailed spectro-electrochemical studies of SeR reveals an intricate electron transfer chain involving the [3Fe–4S], [4Fe–4S], and $Mo^V$ redox centres, and re-oxidation of the Fe–S clusters was observed in the presence of selenate.[40] Although, the enzyme has been crystallized,[41] but its full molecular structure is not known yet. X-ray absorption spectroscopy studies of SeR *T. selenatis* by Pickering, Graham and co-workers suggest a $Mo^V$=O molybdopterin cofactor. In the reduced state, the Mo possesses a des-oxo active site, with also four sulfurs and possibly one oxygen ligand (as shown in Scheme 1).[34] As a result, there has been a keen interest in preparing synthetic model complexes of the Mo active site.[42]

Although a range of different enzymatic biosensors have been reported for detecting environmental contaminants, including organophosphate and carbamate pesticides,[43] toxic metals (arsenic[44] or chromium[45]), and some oxoanion (chlorate,[46] nitrate[47]) at present no biosensor system exists for the detection of selenate. We hypothesized that SeR is a suitable biorecognition element for the design of such a biosensor that lends itself to an electrochemical readout, and the results of our studies are described in this contribution.

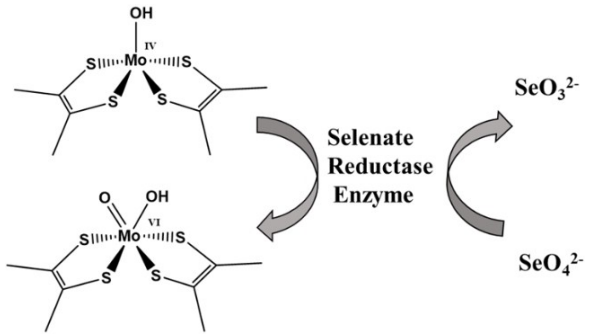


**Scheme 1.** Operation of selenate reductase (SeR) based on structural studies by Pickering, Graham and co-workers of *T. selenatis* SeR showing the active Mo site and its coordination environment and the reduction of selenate, $SeO_4^{2-}$, to selenite, $SeO_3^{2-}$.

## Results and Discussion

### XPS characterization of the surface of gold electrode

Immobilization of the subsequent layers on the gold electrodes was followed by XPS. Figure S1 in the Supporting Information shows XPS spectra of the surface of gold electrode. The presence of sulfur, oxygen, nitrogen and carbon and small amount of iron confirm the immobilization of selenium reductase enzyme on the gold surface. As a result of the Fe and Mo complexes being buried within the film, the observation of Fe and Mo was exceedingly difficult. Table S1 lists the XPS elemental composition for the surface of gold electrode before and after adding SeR. The decrease in the relative amount of the Au 4f peak during immobilization of the subsequent layers confirms the supramolecular protein assembly on the gold electrode.

### ToF-SIMS characterization of the surface of gold electrode

The calibrated positive ion ToF-SIMS spectrum is shown in Figure S2 for the range 0–200 u. No attempt has been made to identify the majority of the fragments which arise from the adsorbed monolayer as we only wish to confirm the presence of both Fe and Mo. The insert in Figure S2 around the Fe clearly confirms its presence giving a measured value of 55.934 u, in good agreement with the theoretical value of 55.936 u (Table S2). Also shown is the Au peak, confirming the accuracy of the calibration (Table S2).

Confirmation of the presence of Mo was more difficult to ascertain due to the proximity of other fragments with similar masses to the Mo isotopes and the weakness of the Mo signal. The negative ion spectrum was used in this case. The isotopic distribution of Mo and MoH (Mo fragment picking up $H^-$) can allow for a confident assignment since it gives rise to peaks at all the nominal masses in the range 92 to 101 u. Figure S3 shows the negative ion spectrum between 0 and 200 u. As before, the accuracy of the calibration is confirmed by the Au peak. Figure S3 also shows the spectra around masses 95, 96, 98, 99, 100 and 101. Plotted on the same scale over a 0.4 u range. The positions of $^n$Mo and $^n$MoH are indicated by arrows and summarized in Table S2. Excellent agreement is obtained with the theoretical values for peak position as are the relative peak intensities lending confidence to the presence of Mo.

### Electrochemical characterization of the surface of gold electrode

Scheme 2 illustrates the stepwise construction of the SeR-modified electrode surface using a lipoic acid active ester approach. After each step, the surface was characterized electrochemically by CV, DPV, and EIS. Figure 1A shows the CVs at a scan rate of 100 mV s$^{-1}$ in the potential window of −0.6 to 1.0 V in 5 mM $[Fe(CN)_6]^{3-/4-}$ in HEPES buffer solution. As the electrode surface is modified, the CV shows a decrease in the current density and an increase in the peak separation (oxidation peak shifts from 0.28 to 0.60 V, reduction peak shifts from 0.08 to −0.45 V). The decrease in the current density as well as the increase in peak separation for $[Fe(CN)_6]^{3-/4-}$ redox couple is the result of increasing film thickness

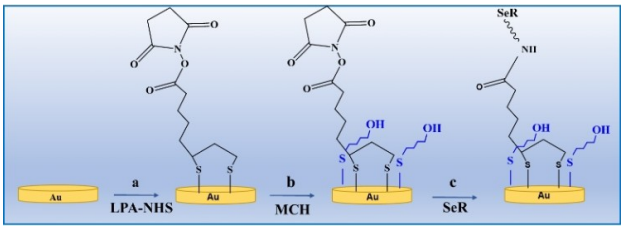


**Scheme 2.** Different steps for modification of the Au electrode. a) The cleaned Au electrode was initially incubated in LPA-NHS (2 mM) incubation for 2 days at 4 °C. b) Afterward it was incubated in MCH (10 mM) solution at room temperature for 15 min. c) The Au electrode was subsequently immersed in the SeR solution (10 ng mL$^{-1}$ in 10 mM PB, pH 7.4) for two days at 4 °C. Finally, the Au-modified electrode was incubated in ethanolamine (100 mM) for 1 h at room temperature before being used to block any unreacted LPA-NHS.

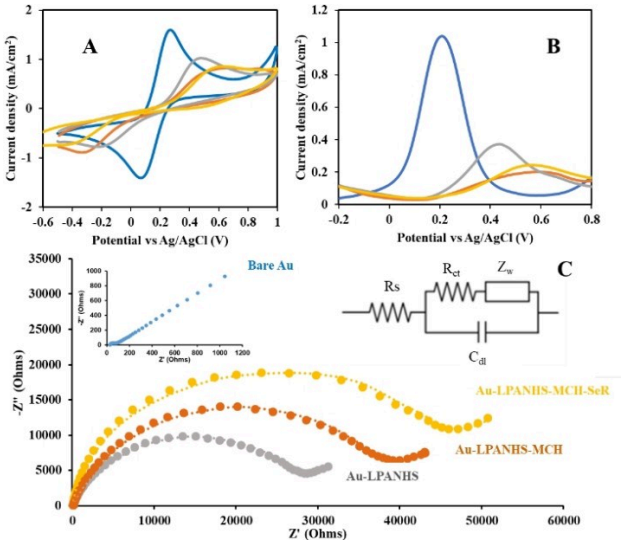


**Figure 1.** Characterization of the gold surface by CV, DPV, and EIS. The measurements were carried out by using a three-electrode system consisting of a Au working electrode, a Pt wire counter electrode, and a Ag/AgCl reference electrode. All measurements were performed in 10 mM HEPES solution (pH 6.0) with 5 mM $[Fe(CN)_6]^{3-/4-}$. The stepwise electrode modification was bare Au electrode (blue), after binding of LPA-NHS (grey), MCH (orange), and selenium reductase (yellow). A) CV, B) DPV, and C) EIS Nyquist plots with (inset) a depiction of the modified Randles' circuit used to analyze the data.

with each of the modification steps. Results obtained by DPV are fully consistent and are shown in Figure 1B. EIS measurements were used to monitor the charge transfer resistance ($R_{ct}$) of the Au electrodes upon modification, and the corresponding Nyquist plots performed at formal potential of $[Fe(CN)_6]^{3-/4-}$ are shown in Figure 1C, where $-Z''$ and $Z'$ are the imaginary and of the real components of the impedance, respectively. As the electrode surface is modified, charge transfer decreases resulting in an increase $R_{ct}$ in EIS. The Nyquist plots in (Figure 1C) clearly exhibit a significant increase in the $R_{ct}$ from 54.6 ± 0.3 Ω (bare gold) to 26.7 ± 0.34 kΩ (for the first step of modification with LIP-NHS) to 45.9 ± 0.34 kΩ (Se–R modified surfaces). The increase from 54.6 Ω to 45.9 kΩ is due to the formation of the Se–R thin film which prevents charge transfer to the electrode surface. The Nyquist plots were analyzed by a modified Randles' equivalent circuit model and shown in the inset of Figure 1C. The Randles' equivalent circuit model is comprised of $R_s$, $R_{ct}$, $C_{dl}$ and $Z_w$, where $R_s$ is the solution resistance, $R_{ct}$ is the charge-transfer resistance, $C_{dl}$ represents the double layer capacitance and $Z_W$ is the Warburg impedance, as result of diffusion of the $[Fe(CN)_6]^{3-/4-}$ redox couple diffusing in and out of the thin film.

### Effect of pH on performance of the SeR-modified electrode in phosphate buffer

Generally, the catalytic activity of redox enzymes is pH dependent,[48] and so it was important to evaluate the pH dependence of the SeR-modified electrodes. For this purpose, electrochemical measurements were carried out at different pH values in 10 mM phosphate buffer (PB). Figure 2A shows CV of SeR-modified electrode in 10 mM PB with pH 7.4 at scan rate 100 mV s$^{-1}$. The CV contains two oxidation peaks at 0.83 and 1.28 V which are associated with the formation of gold oxide and one reduction peak at 0.44 V corresponded to the reduction of the formed gold oxide. In PB with pH 6.0, there is a positive shift for the first oxidation peak to 0.97 V and small negative shift for the second oxidation peak to 1.26 V, there is also a positive shift for reduction peak to 0.49 V (Figure 2B). The current density of oxidation and reduction peaks have been increased by changing pH from 7.4 to 6.0 in PB. In the presence of $SeO_4^{2-}$, there is a new oxidation peak in CV and DPV of SeR-modified electrode that is correlated with the concentration of $SeO_4^{2-}$. CV shows a new oxidation peak at 0.76 V in PB with pH 7.4 and 0.83 V in PB with pH 6.0 (Figure 2A, B). Figure 2C shows the DPV of the SeR-modified electrode in presence of $SeO_4^{2-}$ in 10 mM PB with pH 6.0. The obvious new peak at 0.83 V is related to $SeO_4^{2-}$.

The effect of pH on the peak potential signal showing the electrochemical behavior of the $SeO_4^{2-}$ in the different pHs range of 3.0–7.4 was investigated using DPV. Based on the plot of potential versus pH in Figure 2D, the peak potential of $SeO_4^{2-}$ displayed a negative shift from 1.02 to 0.76 V as pH increases from 3.0 to 7.4. The plot of potential shift versus pH has a slope of 0.0588 V/pH that is very close to theoretical Nernst slope $\left(-\frac{2.303mRT}{nF}\right.$ or 0.059 $\left.\left(\frac{m}{n}\right)\right)$ V/pH, $m$ and $n$ are the numbers of protons and electrons). It shows that the number of hydrogens and the number of electrons involved the redox reaction are equal ($m = n$).

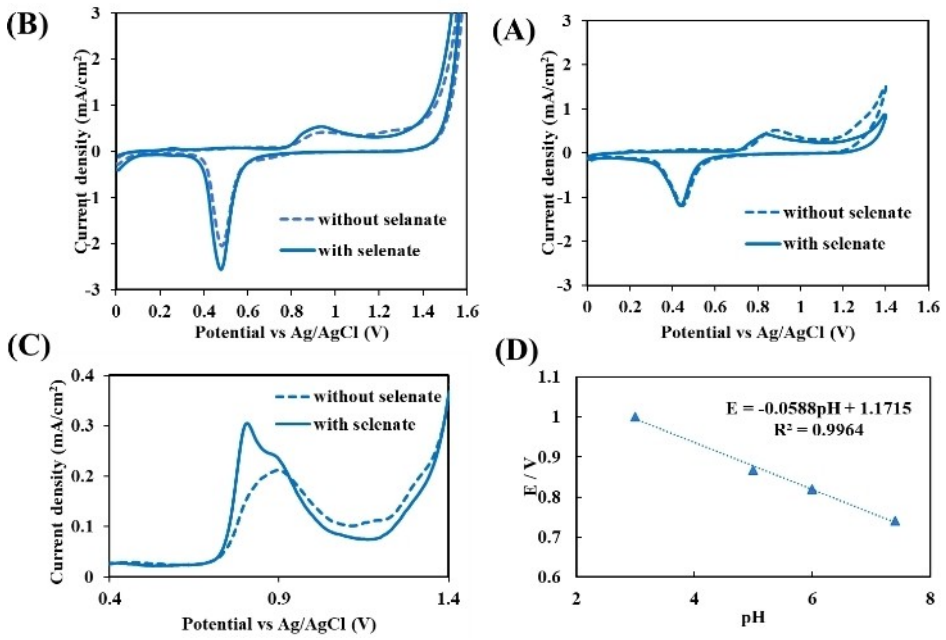


**Figure 2.** CV of SeR-modified electrode in absence and presence of selenate and scan rate 100 mV $s^{-1}$ at A) pH 7.4 and B) pH 6.0. C) DPV of SeR-modified electrode in the absence and presence of selenate at pH 6.0. D) Plot of changing potential vs. pH in presence of $SeO_4^{2-}$. 10 mM PB, $NaClO_4$ 100 mM, $[SeO_4^{2-}] = 3.9$ mg $L^{-1}$.

This is in good agreements with two proton-two electron selenate/selenite redox reaction.

Our results indicate that the maximum response of the SeR-modified electrode is observed at pH 6.0 (Figure S4A). This is in a good agreement with reports by Rech and Macy, who studied the activation of selenate reductase enzyme,[48] and who demonstrated maximum activity for reduction of selenate at pH 6.0.

## Performance of the SeR-modified electrode in different buffers with pH 6.0

In addition of PB buffer, the performance of the SeR-modified modified electrode was studied in Tris, HEPES and MOPS buffer at pH 6.0. Figure 3A shows CV of SeR-modified electrode in 10 mM Tris buffer with pH 6.0 at scan rate 100 mV $s^{-1}$. In comparison with

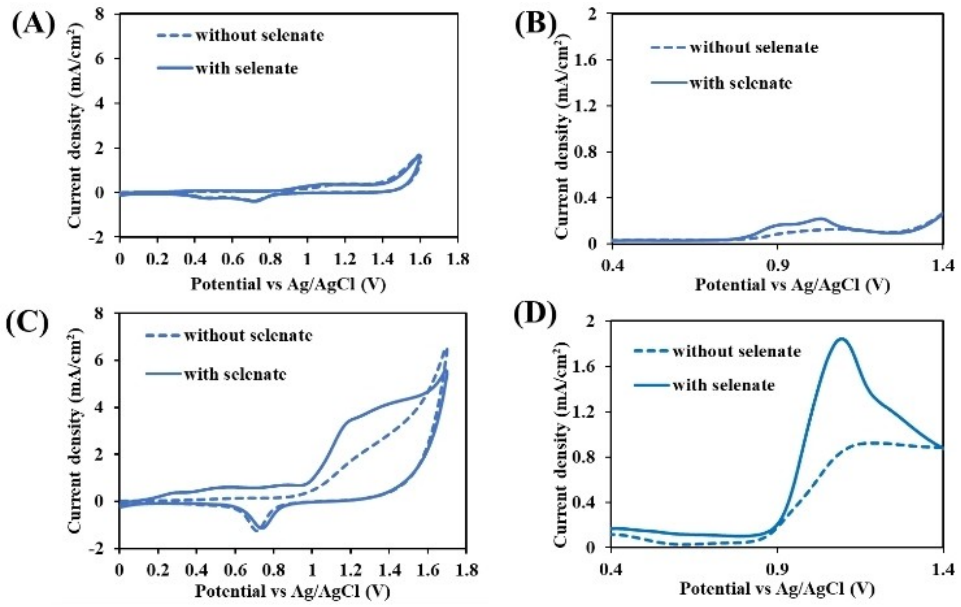


**Figure 3.** A) CV and B) DPV of SeR-modified electrode in 10 mM Tris; C) CV and D) DPV of the SeR-modified electrode in 10 mM HEPES in the absence and presence of selenate. $[SeO_4^{2-}] = 3.9$ mg $L^{-1}$, pH 6.0, 100 mM $NaClO_4$, and scan rate = 100 mV $s^{-1}$.

PB pH 6.0 (Figure 2B), there is only one oxidation peak at 1.12 V but two reduction peaks at 0.72 and 0.47 V. The current density of reduction peaks (0.36 and 0.24 mA cm$^{-2}$) in Tris with pH 6.0 is smaller than that of reduction peak (2.12 mA cm$^{-2}$) in PB with pH 6.0. It shows the reduction of gold oxide occurs in two steps in Tris buffer. In the presence of $SeO_4^{2-}$, CV shows two oxidation peaks, one new peak at 0.98 and other one at 1.07 V and two reduction peaks at 0.72 and 0.47 V (Figure 3A). Two oxidation peaks at 0.91 and 1.01 V are clearly observed in DPV of SeR-modified electrode (Figure 3B). By increasing the concentration of selenate, the current density of the first peak at 0.91 V and the second one at 1.01 V was linearly increased from 0.098 to 0.164 mA cm$^{-2}$ and 0.12 to 0.22 mA cm$^{-2}$, respectively.

Figure 3C shows the CV of SeR-modified electrode in absence and presence of $SeO_4^{2-}$ in 10 mM HEPES buffer with pH 6.0. The CV shows an oxidation signal at 1.3 V and one reduction peak at 0.73 V. After addition of $SeO_4^{2-}$ a new oxidation peak was observed at +1.12 V. And importantly, this particular signal shows a dependence of the peak current intensity with the concentration of $SeO_4^{2-}$. The DPV of SeR-modified electrode in absence and presence of $SeO_4^{2-}$ in 10 mM HEPES buffer with pH 6.0 was shown in Figure 3D, the peak current at +1.12 V increased with addition of $SeO_4^{2-}$.

The current response of SeR modified electrode, $\triangle I$, in different buffers was compared in Figure S4B, the sensor does not exhibit any electrochemical response to selenate in MOPS buffer and displays maximum response in HEPES buffer.

## Response behavior of selenate biosensor

The DPV of SeR-modified electrode with increasing of $SeO_4^{2-}$ concentrations in 10 mM HEPES buffer with pH 6.0 and $NaClO_4$ 100 mM as supporting electrolyte was shown in Figure 4, the peak current at +1.12 V increased with increasing the concentration of $SeO_4^{2-}$ in the range 7.0–3900.0 μg L$^{-1}$. The calibration curve was linear with two segments for concentration ranges of 7.0–580.0 and 580.0–3900.0 μg L$^{-1}$ (Figure 4, inset) of $SeO_4^{2-}$. The limits of detection (LOD) and quantification (LOQ) assessed based on the follow equations LOD = $\frac{3S}{m}$ and LOQ = $\frac{10S}{m}$. In these equations, $S$ and $m$ are the standard deviation of the blank signals ($n$ = 10), and the slope of the linear calibration curve, respectively.[49] Based on these equations, LOD and LOQ were determined to be 4.97 and 15.56 μg L$^{-1}$, respectively.

## Interference study of oxyanions

Rech et al. reported that the presence of nitrate did not inhibit selenate reduction in selenate-grown cells.[48] In addition to nitrate, we investigated the possible interference of other relevant oxyanions $SO_4^{2-}$, $NO_2^-$, $PO_4^{3-}$ and $AsO_4^{3-}$. For this purpose, the response of the biosensor was recorded in $SeO_4^{2-}$ (3.6 mg L$^{-1}$) solution by increasing the concentration of the oxoanion, and the data are reported in Table S3. Our results clearly show that the addition of oxoanions in the different mole ratios ($X^{n-}$/$SeO_4^{2-}$) in the ranges from 0.2 to 100 did not significantly affect the response ($\triangle I$) of the SeR-modified electrodes.

## Response of the SeR-modified electrode for the detection of different oxoanions

The response of the SeR-modified electrode to different oxoanions ($SeO_4^{2-}$, $AsO_4^{3-}$, $SO_4^{2-}$, $PO_4^{3-}$, $NO_3^-$, $NO_2^-$) over a range of 7.0 to 3900.0 μg L$^{-1}$ was studied. Figure 5 shows the response of the SeR-modified electrode at 3900.0 μg L$^{-1}$ of the oxoanions in HEPES at pH 6.0 (Figure S5). Our data indicate that the modified surface shows only a negligible response from other oxyanions, which does not interfere with selenate quantification. This is in a good agreement with reported result of Schroder et al. which showed the purified selenate reductase from *T. selenatis* is specific to selenate.[38]

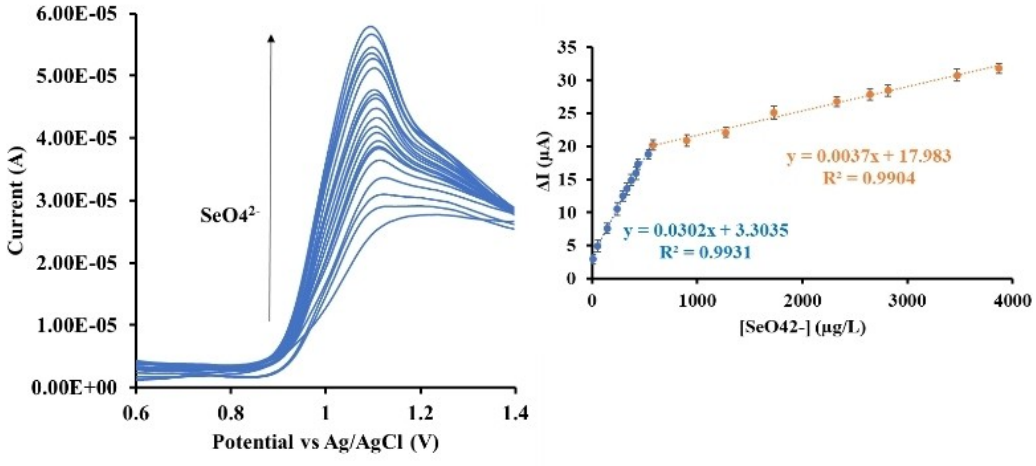


**Figure 4.** Electrochemical response of SeR-modified Au electrodes as a function of increasing $SeO_4^{2-}$ concentration. DPV of a SeR-modified Au electrode at $SeO_4^{2-}$ concentrations from 7.0–3900.0 μg L$^{-1}$ in 10 mM HEPES with pH 6.0, and $NaClO_4$ 100 mM. Inset: calibration curve for $SeO_4^{2-}$.

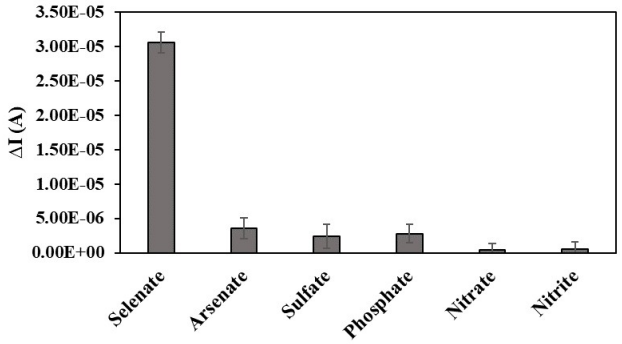


**Figure 5.** Response of the SeR-modified surface to different oxoanions ($SeO_4^{2-}$, $AsO_4^{3-}$, $SO_4^{2-}$, $PO_4^{3-}$, $NO_3^-$, $NO_2^-$) at 3900 μg L$^{-1}$ of the oxyanion in HEPES at pH 6.0.

**Table 1.** Determination of $SeO_4^{2-}$ the domestic water and wastewater samples.

| Sample | Detected [μg L$^{-1}$] | Spiked [μg L$^{-1}$] | Found ± S [μg L$^{-1}$] | Relative recovery [%] |
|---|---|---|---|---|
| domestic | – | 25 | 23.8 ± 1.1 | 95.2 |
| wastewater | | 200 | 204.7 ± 3.5 | 102.4 |
| river water | – | 25 | 25.5 ± 0.91 | 102.0 |
| | | 200 | 203.5 ± 2.3 | 101.8 |
| creek water | – | 25 | 24.2 ± 1.2 | 96.8 |
| | | 200 | 198.5 ± 2.5 | 99.3 |

### Stability, reproducibility, and repeatability the biosensor electrode

The stability and reproducibility of the SeR-modified surface for selenate detection was studied for ten successive determinations ($n = 11$). DPVs of $SeO_4^{2}$ (3.6 mg L$^{-1}$, HEPES, pH 6.0) shown in Figure S6A. The relative standard deviation was calculated to be 2.17%. The long-term stability of the biosensor was also tested by recording DPVs of the biosensor electrode in a period of 15 days upon storage at 4 °C and subsequent analysis of $SeO_4^{2-}$. The 10% loss of activity ($SeO_4^{2-}$ reduction) was observed after 7 days and the activity of biosensor was decreased to 60% after 15 days. The response of the SeR-modified electrodes decreases as the electrode ages. This can be due to decay in enzyme activity over time. The decay of enzyme activity over time has been reported before in unrelated enzymatic biosensors.[46] But interestingly, the biosensor is stable at room temperature for several measurements and it is possible to store it at 4 °C for up to 7 days without loss of sensitivity.

The repeatability of the SeR-modified electrode was tested for the six individual electrodes for $SeO_4^{2}$ (3.9 mg L$^{-1}$) and the results are shown in Figure S6B. The relative standard deviation for these six electrodes was calculated 2.77%. Our results clearly showed the excellent stability, reproducibility, and repeatability of the biosensor system for determination of selenate oxoanion.

### Determination of $SeO_4^{2-}$ in real samples

SeR-modified electrode was tested for the determination of $SeO_4^{2-}$ in real samples domestic water and wastewater. The samples were investigated by diluting them four times using HEPES buffer with pH 6.0, and the standard addition technique was utilized for the determination of $SeO_4^{2-}$ using DPV technique. As shown in Table 1, the results with a satisfactory relative recovery of three target analytes in all samples indicated that the sensor was capable of selectively detecting the analytes even in the presence of complex real-sample matrixes. The $SeO_4^{2-}$ was not pre-existing in any of the tested matrixes. The recovery values between 95.2 and 102.4% were all within the acceptable range. These results indicated the developed modified electrode had promising potential for the determination of $SeO_4^{2-}$ in real samples.

### Comparisons to electrochemical methods

Table 2 compares the figures of merit of the SeR-modified electrode with the recently available values in the literature related to the determination of Se. Based on Table 2, the analytical performance of our SeR-modified electrode in both linear range and limit of detection (LOD) are comparable or better than the ones recently published in the literature.[50–55] In addition, the conditions for determination of selenate in this study are very mild in comparison to others that used high concentration of acid,[50] or

**Table 2.** Figures of merit of the proposed Au biosensor electrode in comparison with the recently reported modified electrodes in literature for determination of Se.

| Modified electrode | Technique | pH/condition | Linear range [μg L$^{-1}$] | LOD [μg L$^{-1}$] | Ref. |
|---|---|---|---|---|---|
| mercury-graphite electrode | cathodic square-wave voltammetry | 6 M HCl | 2.5–40 | – | 50 |
| thick-film graphite-containing gold electrode | anodic differential pulse voltammetry | 0.1 M $HClO_4$ solution | 0–50 | 0.1 | 51 |
| Au-modified boron-doped diamond electrode | CV | 0.1 M $HClO_4$ | 2000–10000 | 50 | 52 |
| screen printed graphite macro electrodes | anodic stripping voltammetry | 0.1 M $HClO_4$ | 10–1000 | 4.9 | 53 |
| gold ultramicroelectrodes | square wave anodic stripping voltammetry | 0.005 M $H_2SO_4$ | 0–500 | 0.42 | 54 |
| modified graphite electrode with diazonium salt | DPV | electrolyte 0.6 M HCl + $Cu^{2+}$ (100 mg l$^{-1}$) + $Hg^{2+}$ (100 mg l$^{-1}$) | 200–$4.0\times10^6$ | 57 | 55 |
| SeR-modified Au electrode | DPV | 10 mM HEPES with pH 6 | 7.0-3900 | 4.9 | this work |

using very strong acids at significantly lower pH (e.g., $HClO_4$, 0.1 M);[51–53] $H_2SO_4$, 0.005 M;[54] HCl, 0.6 M).[55] Also, there is no need to do any stripping step, which adds additional time to the measurement.[53,54]

## Conclusion

For the first time, a bacterial enzyme-based selenate reductase sensor is introduced that allows the electrochemical detection of selenate oxoanion. The gold biosensor is efficient, sensitive and stable for the detection of $SeO_4^{2-}$. The maximum response of the biosensor for the detection of selenate was observed in HEPES buffer at pH 6.0. The electrode exhibited a good response to changes in selenate concentration over 7.0–3900.0 $\mu g L^{-1}$ and provided LOD and LOQ values of 4.97 and 15.56 $\mu g L^{-1}$, respectively. Our inference study shows that $SO_4^{2-}$, $NO_3^-$, $NO_2^-$, $PO_4^{3-}$ and $AsO_4^{3-}$ oxoanions do not interfere in the detection of selenate. This study shows that the biosensor is specific for the detection of selenate oxoanion. The biosensor has a recovery of selenate between 95.2–102.4% in different real water samples, and is thus a promising platform for the development of sensitive biosensor for the detection of selenate in real samples.

## Experimental Section

**Material**: Selenium reductase enzyme (SeR) was purchased from Creative Enzymes NY, www.creative-enzymes.com/about.html. Tris (tris(hydroxymethyl)aminomethane), HEPES (4-(2-hydroxyethyl)-1-piperazineethanesulfonic acid), and MOPS (3-(*N*-morpholino)propanesulfonic acid) were purchased from BioShop (Toronto, ON, www.bioshopcanada.com). All buffers with concentration of 10 mM were prepared with Milli-Q water. Lipoic acid *N*-hydroxysuccinimide ester (LPA-NHS) was purchased from Synchem UG & Co. Sodium salts ($Na_2SeO_4$, $Na_3AsO_4$, $Na_3PO_4$, $Na_2SO_4$, $NaNO_3$, and $NaNO_2$), mercaptohexanol (MCH), ethanolamine and all other chemicals were purchased from Sigma-Aldrich unless otherwise specified and used as received.

**X-ray photoelectron spectroscopy**: X-ray photoelectron spectroscopy (XPS) measurements were obtained using the K-Alpha XPS spectrometer (Thermo Fisher Scientific) located at the Ontario Centre for the Characterisation of Advance Materials (OCCAM). Survey spectra (nominal 400 μm spot, 200 eV pass energy (PE), 1 eV step size) were obtained for all samples followed by low resolution spectra (150 eV pass energy, 0.2 eV step size) on the spectral regions of interest (Au 4f, C 1s, N 1s, O 1s, S 2p, Fe 2p and Mo 3d) from which the composition was obtained. High-resolution spectra were obtained also for the Au, C and O (PE = 25 eV, 0.1 eV step-size) as well as for N 1s (PE = 40 eV, 0.15 eV step-size). Acquisition times and PE being adjusted to optimise S/N while maintaining a reasonable collection time. Charge compensation was applied using the system's combined $e^-/Ar^+$ flooding source, with the energy scale adjusted to place the Au $4f_{7/2}$ at 84.0 eV. All data processing was performed using the software supplied with the system (Avantage 5.957). Composition (relative atomic%) was obtained from the individual region spectra after subtraction of a modified Shirley-type[56] background (designated "Smart" in the software) and application of the supplied sensitivity factors (Au 4f–20.735, C 1s–1.000, O 1s–2.881, N 1s–1.676, S 2p–1.881 and Fe 2p–14.353).

**Time-of-flight secondary ion mass spectroscopy (ToF-SIMS)**: Both positive and negative ion spectra were obtained on an IONTOF TOFSIMS V (IONTOF GmbH, Münster, Germany) located at OCCAM. $Bi^{3+}$ (30 keV energy) primary ions were rastered over an area of 500 μm × 500 μm to generate the spectra in a high mass resolution mode with charge neutralisation applied in between the primary beam pulses.[57] An acquisition time of 100 s was used, well below the static limit.[57] Spectra were calibrated by assigning the mass values to progressively identified peaks which included H, $CH_3$, Na, Si and so on for the positive spectra, and C, $C_2$, $C_3$ and $C_4$ for the negative spectra. Because we were looking for monolayer adsorption, no attempt was made to clean the sample, even with the system's Ar cluster source.

**Electrochemical measurements**: Cyclic voltammetry (CV), differential pulse voltammetry (DPV), and electrochemical impedance spectroscopy (EIS) measurements were recorded on a CHI-660 C electrochemical station (CH Instruments, Austin, Texas) with an enclosed Faraday cage. The electrochemical cell was a conventional three-electrode two compartment system consisting of a SeR-modified Au electrode as working electrode, a platinum wire as an auxiliary electrode, and an Ag/AgCl (KCl, 3 M) as reference electrode. The cathodic and anodic cells were separated by a $KNO_3$ salt bridge connecting the two compartments to prevent potential cross-contamination. In all experiments, CVs started at the open circuit potential with a 30 s quiet time followed by a positive scan polarity from 0.0 to 1.6 V vs. Ag/AgCl at scan rate 100 $mV s^{-1}$. For DPV measurements, the potential was scanned in a wide potential from 0.4 to 1.4 V vs. Ag/AgCl with a step potential of 4 mV, a modulation time of 0.05 s, an interval time of 0.5 s and a pulse amplitude of 25 mV. EIS was used to characterize and monitor the step-by-step construction of the sensing surface. All EIS measurements were carried out in 10 mM HEPES buffer, pH 6.0, in the presence of 5.0 mM $[Fe(CN)_6]^{3-/4-}$ over a frequency range of 0.1 Hz to 100 kHz with an AC amplitude of 0.005 V amplitude and a 5 s quiet time at 0.25 V potential of $[Fe(CN)_6]^{3-/4-}$. The Nyquist plots were analyzed by a modified Randles' equivalent circuit model using the ZSimpWin 2.0 software.

**Preparation of modified gold electrodes**: Before modification, the bare gold electrodes (2 mm diameter) were immersed in a piranha solution ($H_2SO_4/H_2O_2$ 3:1, *v/v*) for 30 s to remove organic contaminants in the surfaces and rinsed with Milli-Q water with a resistivity of 18.2 MΩ cm. The bare gold electrodes were mechanically polished using aqueous alumina slurries of 1, 0.3 and 0.05 μm for 5 min each in sequence. Next, the electrodes were sonicated in Milli-Q water for 15 min and then in ethanol for another 5 min. After the mechanical cleaning, the Au electrode subjected to electrochemical cleaning in 0.5 M KOH (50 times scan from −2.0 to 0.0 V Ag/AgCl with a scan rate of 100 $mV s^{-1}$), rinsed with water, and subsequently cleaned in 0.5 M $H_2SO_4$ (50 times scan from 0.0 to1.5 V Ag/AgCl with a scan rate of 100 $mV s^{-1}$).The cleaned Au electrodes were immediately incubated in ethanolic solution of LPA-NHS (2 mM, 50 μL) at 4 °C for 72 h. Next, the electrodes were immersed in mercaptohexanol (10 mM in 10 mM phosphate buffer with pH 7.4) for 15 mins at room temperature to block pinholes on the Au surface. Then, the electrodes were incubated in a solution of SeR (10 $ng mL^{-1}$ in phosphate buffer 10 mM, pH 7.4) at 4 °C for 48 h. Finally, the electrodes were immersed in ethanolamine (100 mM, in 10 mM phosphate buffer with pH 7.4) for 1 h before use to block any unreacted LPA-NHS. After each step the electrodes were thoroughly washed with phosphate buffer (10 mM, pH 7.4). Scheme 2 illustrates the construction of the sensor surfaces in the stepwise fashion.

## *Acknowledgements*

This work was supported by the ANatural Sciences and Engineering Research Council of Canada (NSERC-DG-2016-06122), and the University of Toronto.

## Conflict of Interest

The authors declare no conflict of interest.

## Data Availability Statement

The data that support the findings of this study are available from the corresponding author upon reasonable request.

**Keywords:** enzymatic biosensors · selenium reductase · selenates · electrochemistry

[1] F. E. Huggins, C. L. Senior, P. Chu, K. Ladwig, G. P. Huffman, *Environ. Sci. Technol.* **2007**, *41*, 3284–3289.
[2] Y. V. Nancharaiah, P. N. L. Lensa, *Microbiol. Mol. Biol. Rev.* **2015**, *79*, 61–80.
[3] C. Herrero Latorre, J. Barciela García, S. García Martín, R. M. Peña Crecente, *Anal. Chim. Acta* **2013**, *804*, 37–49.
[4] A. M. Brasher, R. S. Ogle, *Arch. Environ. Contam. Toxicol.* **1993**, *24*, 182–186.
[5] P. L. Orr, K. R. Guiguer, C. K. Russel, *Ecotoxicol. Environ. Saf.* **2006**, 63, 175–188.
[6] R. S. Ogle, K. J. Maier, P. Kiffney, M. J. Williams, A. Brasher, L. A. Melton, A. W. Knight, *Lake Reservoir Manage.* **1988**, *4*, 165–173.
[7] D. B. D. Simmons, D. Wallschläger, *Environ. Toxicol. Chem.* **2005**, 1331–1343.
[8] H. Morlon, C. Fortin, M. Floriani, C. Adam, J. Garnier-Laplace, A. Boudou, *Aquat. Toxicol.* **2005**, *73*, 65–78.
[9] a) G. F. Riedel, D. P. Ferrier, J. G. Sanders, *Water Air Soil Pollut.* **1991**, *57–58*, 23–30; b) J. M. Besser, T. J. Canfield, T. W. Lapoint, *Environ. Toxicol. Chem.* **1993**, *12*, 57–72; c) J. Li, G. Loi, L. Otero-Gonzalez, G. Du Laing, I. Ferrer, P. N. L. Lens, *Water Sci. Technol.* **2020**, *81*, 1852–1862.
[10] I. S. Palmer, O. E. Olson, *J. Nutr.* **1974**, *104*, 306–314.
[11] a) G. F. Kramer, B. N. Ames, *Mutat. Res.* **1988**, *201*, 169–180; b) M. Björnstedt, S. Kumar, A. Holmgren, *J. Biol. Chem.* **1992**, *267*, 8030–8034.
[12] a) S. Kumar, M. Björnstedt, A. Holmgren, *Eur. J. Biochem.* **1992**, *207*, 435–439; b) Y. Zou, P. Niu, J. Yang, J. Yuan, T. Wu, X. Chen, *Biol. Ther.* **2008**, *7*, 689–696.
[13] G. Peyroche, C. Saveanu, M. Dauplais, M. Lazard, F. Beuneu, L. Decourty, C. Malabat, A. Jacquier, S. Blanquet, P. Plateau, *PLoS One* **2012**, *7*, e36343.
[14] P. Bao, Z. Chen, R.-Z. Tai, H.-M. Shen, F. L. Martin, Y.-G. Zhu, *J. Proteome Res.* **2015**, *14*, 1127–1136.
[15] FAO/WHO, *Vitamin and Mineral Requirements in Human Nutrition*, 2nd ed. *Report of a Joint FAO/WHO Expert Consultation*, Bangkok, Thailand, 21–30 September 1998, World Health Organization, Geneva, **2004** (http://whqlibdoc.who.int/publications/2004/9241546123.pdf).
[16] World Health Organization, *Guidelines for Drinking-Water Quality*, First addendum to third edition, Geneva, **2006**, *1*, 433–434.
[17] K. Shrivas, D. K. Patel, *Food Chem.* **2011**, *124*, 1673–1677.
[18] B. Gammelgaard, O. Jøns, *J. Anal. At. Spectrom.* **2000**, *15*, 945–949.
[19] B. Chen, M. He, X. Mao, R. Cui, D. Pang, B. Hu, *Talanta* **2011**, *83*, 724–731.
[20] S. Dilli, I. Sutikno, *J. Chromatogr. A* **1984**, *300*, 265–302.
[21] R. Gurkan, H. I. Ulusoy, M. Ackcay, P. Bulut, *Rare Met.* **2011**, *30*, 477–487.
[22] a) M. Rievaj, E. Culková, D. Šandorová, Z. Lukáčová-Chomisteková, R. Bellová, J. Durdiak, P. Tomčík, *Molecules* **2021**, *26*, 1768; b) J. Filip, Š. Vinter, E. Čechová, J. Sotolářová, *Analyst* **2021**, *146*, 6394–6415.
[23] S. Goldberg, D. A. Martens, H. S. Forster, M. J. Herbe, *Soil Sci. Soc. Am. J.* **2006**, *70*, 41–47.
[24] D. Sanchez-Rodas, F. Mellano, E. Morales, I. A. Giraldez, *Talanta* **2013**, *106*, 298–304.
[25] F. Bettazzi, D. Voccia, A. Bencini, C. Giorgi, I. Palchetti, B. Valtancoli, L. Conti, *Eur. J. Inorg. Chem.* **2018**, *23*, 2675–2679.
[26] R. S. Posey, R. W. Andrews, *Anal. Chim. Acta* **1981**, *124*, 107–112.
[27] R. W. Andrews, D. C. Johnson, *Anal. Chem.* **1975**, *47*, 294–299.
[28] P. Zuman, G. Somer, *Talanta* **2000**, *51*, 645–665.
[29] V. Beni, G. Collins, D. W. M. Arrigan, *Anal. Chim. Acta* **2011**, *699*, 127–133.
[30] H. S. Tan, S. P. Kounaves, *Electroanalysis* **1998**, *10*, 364–368.
[31] B. Lange, C. M. B. van den Berg, *Anal. Chim. Acta* **2000**, *418*, 33–42.
[32] N. Y. Stohzhko, Z. V. Shalgyna, N. A. Malakhova, *J. Anal. Chem.* **2004**, *59*, 374–380.
[33] C. F. Pereire, F. B. Gonzaga, A. M. Guarita-Santos, J. R. De Souza, *Talanta* **2006**, *69*, 877–881.
[34] M. J. Maher, J. Santini, I. J. Pickering, R. C. Prince, J. M. Macy, G. N. George, *Inorg. Chem.* **2004**, *43*, 402–404.
[35] C. M. Debieux, E. J. Dridge, C. M. Mueller, P. Splatt, K. Paszkiewicz, I. Knight, H. Florance, J. Love, R. W. Titball, R. J. Lewis, D. J. Richardson, C. S. Butler, *Proc. Natl. Acad. Sci. USA* **2011**, *108*, 13480–13485.
[36] M. Bébien, J. Kirsch, V. Méjean, A. Verméglio, *Microbiology* **2002**, *148*, 3865–3872.
[37] Y. Tan, R. Yao, R. Wang, D. Wang, G. Wang, S. Zheng, *Microb. Cell Fact.* **2016**, *15*, 157.
[38] a) I. Schroder, S. Rech, T. Krafft, J. M. Macy, *J. Biol. Chem.* **1997**, *272*, 23765–23768; b) C. Kisker, H. Shindelin, D. C. Rees, *Annu. Rev. Biochem.* **1997**, *66*, 233–267; c) R. Hille, *Chem. Rev.* **1996**, *96*, 2757–2816.
[39] J.-J. Wang, C. Tessier, R. H. Holm, *Inorg. Chem.* **2006**, *45*, 2979–2988.
[40] a) E. J. Dridge, C. A. Watts, B. J. Jepson, K. Line, J. M. Santini, D. J. Richardson, C. S. Butler, *Biochem. J.* **2007**, *408*, 19–28; b) E. C. Lowe, S. Bydder, R. S. Hartshorne, H. L. U. Tape, E. J. Dridge, C. M. Debieux, K. Paszkiewicz, I. Singleton, R. J. Lewis, J. M. Santini, D. J. Richardson, C. S. Butler, *J. Biol. Chem.* **2010**, *285*, 18433–18442.
[41] M. J. Maher, J. M. Macy, *Acta Crystallogr. Sect. D* **2002**, 58, 706–708.
[42] J.-J. Wang, C. Tessier, R. H. Holm, *Inorg. Chem.* **2006**, *45*, 2979–2988.
[43] J. Cao, M. Wang, H. Yu, Y. She, Z. Cao, J. Ye, A. M. Abd El-Aty, A. Hacımüftüo˘glu, J. Wang, S. Lao, *Pesticides. J. Agric. Food Chem.* **2020**, *68*, 7298–7315.
[44] J. Berberich, T. Li, E. Sahle-Demessie in *Separation Science and Technology, Vol. 11* (Ed.: S. Ahuja,), Academic Press, Cambridge, MA, **2019**, Chapter 11.
[45] P. Biswas, A. K. Karn, P. Balasubramanian, P. G. Kale, *Biosens. Bioelectron.* **2017**, *94*, 589–604.
[46] B. C. Okeke, G. Ma, Q. Cheng, M. E. Losi, W. T. Frankenberger, *J. Microbiol. Methods* **2007**, *68*, 69–75.
[47] J. W. Aylott, D. J. Richardson, D. A. Russell, *Analyst* **1997**, *122*, 77–80.
[48] S. A. Rech, J. M. Macy, *J. Bacteriol.* **1992**, 7316–7320.
[49] J. C. Miller, J. N. Miller, *Statistics for Analytical Chemistry*, 2nd ed., Wiley, New York, **1988**.
[50] O. G. Filichkina, E. A. Zakharova, G. B. Slepchenko, *J. Anal. Chem.* **2004**, *59*, 481–486.
[51] N. Yu, Stozhko, Zh. V. Shalygina, N. A. Malakhova, *J. Anal. Chem.* **2004**, *59*, 374–380.
[52] T. A. Ivandini, Y. Einaga, *Electrocatalysis* **2013**, *4*, 367–374.
[53] A. V. Kolliopoulos, J. P. Metters, C. E. Banks, *Anal. Methods* **2013**, *5*, 851–856.
[54] S. H. Tan, S. P. Kounaves, *Electroanalysis* **1998**, *10*, 364–368.
[55] G. B. Slepchenko, E. S. Moiseeva, E. V. Dorozhko, M. S. Ostapenko, O. L. Mezentseva, A. Auelbekova, F. K. Njung, *Anal. Methods* **2021**, *13*, 1584–1590.
[56] D. A. Shirley, *Phys. Rev.* **1972**, *55*, 4709–4714.
[57] R. N. S. Sodhi, *Analyst* **2004**, *129*, 483–487.

Manuscript received: March 28, 2022
Accepted manuscript online: June 24, 2022
Version of record online: July 26, 2022